Theoretical study of the *syn* and *anti* thiophene-2-aldehyde conformers using density functional theory and normal coordinate analysis

Guillermo Diaz Fleming [a,*], Rainer Koch [b], M.M. Campos Vallete [c]

[a] *Department of Chemistry, University of Playa Ancha, Valparaiso, Casilla 34-V, Chile*
[b] *Institute for Pure and Applied Chemistry, University of Oldenburg, P.O. Box 2503, D-26111 Oldenburg, Germany*
[c] *Molecular Spectroscopy Laboratory, Department of Chemistry, Faculty of Science, University of Chile, Casilla 653, Santiago, Chile*

Abstract

An extensive computational study of thiophene-2-aldehyde conformers *syn* and *anti* has been carried out using density functional (DFT). From these calculations, B3LYP/6-31G(d) has been chosen as it produces results remarkably close in comparison with experimental ones, with less demanding computational time. Data obtained from DFT computation were used to perform a normal coordinate analysis to complement and give insight in the experimental vibrational assignment. Calculated dipole moments and relative stabilities of isomers coherently support experimental statements given in the literature.

Keywords: Thiophene-2-aldehyde; Conformers; DFT; Normal coordinate analysis

1. Introduction

The use of computational techniques is becoming increasingly common throughout all the various fields of chemistry [1]. This can be largely attributed to the increasing availability of robust energy derivative programs, in which first and second energy derivatives are computed analytically [2], that is, the energy gradient has greatly improved the efficiency and reliability of geometry optimization of ab initio molecular orbital methods. Taking into account that optimization methods that use gradients require an initial estimate of the Hessian or second derivative matrix, underlines the importance of an accurate estimate as it would lead to a more rapid convergence.

The main purpose of this work is to take advantage of the quantum mechanics to support and complement experimental data. In this sense, we have considered the different structural and energetic implications in the study of conformational systems. Thus, the preference between two possible planar conformations in the study of monosubstituted heterocycles such as thiophene is often strongly medium-dependent because of their differing polarities. The conformational preferences of these molecules have, during the last few years, attracted much attention, with virtually the complete armory of physical-organic chemistry being brought to bear the problem. In these circumstances, the conformational preference in the absence of solvent is of some importance. Ab initio molecular orbital theory provides a means of determining intrinsic conformational preferences and is suitable to study physical properties and vibrational characteristics of conformers arising from the molecular structure and conformational equilibrium.

When thermodynamic parameters as well as infrared and Raman spectra of conformers are determined experimentally procedures, the quality of different ab initio methods can be tested by comparison with experimental results. This work was performed to identify a suitable computational method for treating conformers of thiophene derivatives on the basis of experimental data of thiophene-2-aldehyde obtained by electron diffraction and microwave, infrared, Raman and matrix isolation spectroscopy [3]. This work will reveal additional quantitative chemical knowledge of the formation, relative stability, geometry, as well as giving more detailed insight into systematic differences between calculation and experiment in the assignment of vibrational spectra, through the calculated force field and potential energy distribution of the corresponding normal modes.

* Corresponding author. Tel.: +56 32 500276; fax: +56 32 347688.
E-mail address: guillermodiaz@upa.cl (G.D. Fleming).

Among the distinct ab initio methods, one of the most popular is that concerning to Hartree–Fock calculations, which treat the electrons as individual wave functions. However, electrons do not act independently of each others and to improve results the electron correlation must be taken by mixing in excited state wave functions with ground state wave functions.

Density functional theory (DFT) takes another approach. The interaction system of electrons is approximated by using a function to describe the electron density (a functional) rather than individual wave functions for each of the electrons [4]. That is, DFT relies on the total electron density, with the electron "placed" in non-interacting Kohn–Sham (KS) orbitals [5]. There are some results indicating that the vibrational frequencies and intensities from DFT calculations are better than those obtained from second order Møller–Plesset (MP2) perturbation theory [6]. With the DFT approach it is possible to perform calculations of large molecules because the potential depends on three spatial coordinates rather than 3*N* degrees of freedom.

On the other hand, application of DFT [7–10] to chemical systems has received much attention recently because of a faster convergence in time than traditional quantum mechanical correlation methods in part, and improvements in the prediction of the molecular force field, vibrational frequencies (and consequently thermodynamic parameters), dipole moments and polarizability data. Therefore, the force field from DFT calculation could be utilized with the spectroscopic data for the assignment of observed frequencies and the refinements of molecular force field under study.

2. Computational details

The calculations in this study were performed using the Gaussian '03 suite of programs [11]. Several DFT methods have been evaluated, they consisted of the S-VWN local functional, corresponding to the Slater–Dirac exchange functional (S) [12] with the Vosko–Wilk–Nusair fit for the correlation functional (VWN) [13], the BLYP gradient-corrected functional, corresponding to Becke's gradient corrected exchange functional (B) [14] with the Lee–Yang–Parr fit for the correlation functional (LYP) [15] and two hybrid functional B3LYP and B3PW91, corresponding to Becke's three parameter exchange functional (B3) [16] with the LYP correlation functional and with Perdew and Wang's gradient-corrected correlation functional (PW91) [17]. With respect to geometry and vibrations, only small differences are observed for the different functionals, so that we limit the study to the best-known B3LYP hybrid functional.

Basis set dependence for the density functional was investigated by systematically adding polarization function to split valence basis sets, such as 6-31G(d,p) [18], 6-311G(d,p) and 6-31G(d) [19–21]. Again, no significant differences were observed, so that for subsequent calculations the well-known B3LYP/6-31G(d) level of theory is employed which also gives the best agreement for vibrations with the experimental data.

Results of the other level of calculation are presented in Appendix A (Table A1). The harmonic vibrational frequencies and eigenvectors as well as infrared intensities were subsequently calculated using the analytical second derivatives for ab initio methods and numerical differentiation of analytical gradients for the functionals, while Raman intensities which depend on the square of the polarizabilitiy derivatives require the calculation of the third derivative of the system energy with respect to coordinates and electric field. In order to account for an harmonic behavior, the obtained frequencies are scaled with a factor of 0.9614. This value has been applied to all regions of the spectrum, so it is possible that some vibrations are affected more significantly than others [22].

Those force constants obtained in Cartesian coordinates with Gaussian were transformed into internal force constants through FCART 01, which is a modification of a previous software [23] written to accomplish all the necessary transformation and calculations using the G03 output. It extracts from the G03 archive file the calculated geometry (including atom type and number sequencing), Cartesian force constants, dipole moment and polarizability derivatives to produce the calculated frequencies, intensities, depolarization ratios and statistics. With this program we have also obtained the matrices of the potential energy distribution (PED) which provide a measure of each internal coordinate's contribution to the normal coordinate at the above mentioned theory level.

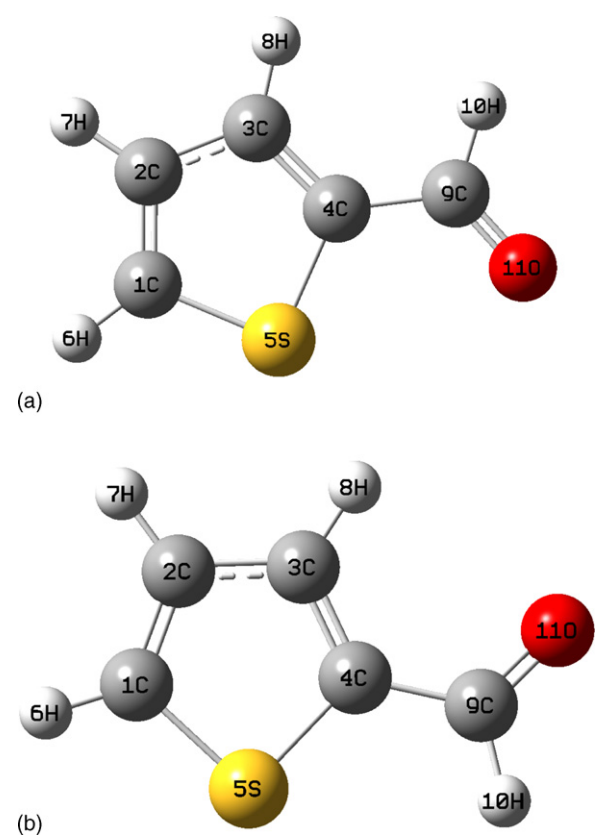

Fig. 1. Diagram of the *syn* (a) and *anti* (b) thiophene-2-aldehyde conformers.

3. Results and discussion

3.1. Geometrical structure

The optimized *syn* and *anti* conformers are presented in Fig. 1. Selected geometrical data are given in Table 1 together with the experimental values determined in Ref. [3]. In general, the agreement between our results and the experimental ones is quite good, giving the first indication of the quality of the actual level of calculation. Our calculations show planar structures for both conformers, complementing the study in Ref. [3], in which such a structure has only been detected for the *syn* isomer which is the predominant isomer. Additionally, these results are consistent with partial conjugation in the bond between atoms 2 and 3 (opposite to the sulfur atom) in the thiophene ring (see Fig. 1), which in turn is a consequence of the addition of the aldehyde molecule, which is a π-electron-withdrawing. In general there is no significant difference between the geometrical parameters of both conformers observed. The *syn* and *anti* structures are characterized by the small difference of the geometrical parameters, as well as in the slightly different Mulliken atomic charges (Table 2), in particular those concerning sulfur and oxygen.

3.2. Vibrations

The scaled calculated harmonic frequencies and the experimental ones reported in Ref. [3] are given in Table 3, while infrared and Raman intensities of the calculated frequencies are collected in Table 4. The simulated infrared and Raman spectra for both conformers are presented in Fig. 2. There is generally excellent agreement between the theoretical and experimental data, differences usually only a few wave numbers, both for *syn* and *anti* conformations of thiophene-2-aldehyde.

The most intensive infrared bands for the *syn* conformer are calculated at 2813 and 1711 cm^{-1}, in agreement with groups of bands at about 2800 and 1705 cm^{-1}, assigned experimentally in Ref. [3] to this conformer. Concerning the calculated

Table 1
Experimental [3] and calculated geometrical parameters distances (Å) angles (°)

	Exp.	*syn*	*anti*	Atoms
Bond lengths				
C–H	1.114	1.085	1.084	(3,8)
		1.112	1.111	(9,10)
		1.084	1.084	(2,7)
		1.083	1.082	(1,6)
C=O	1.224	1.219	1.218	
C–S	1.717	1.727	1.725	(1,5)
		1.746	1.726	(4,5)
C=C	1.375	1.380	1.379	(3,4)
		1.374	1.375	(1,2)
C–C	1.431	1.419	1.417	(2,3)
C–(CHO)	1.466	1.458	1.464	
Bond angles				
C=C–CHO	126.4	127.573	127.274	
C–C–C	112.2 (ring)	112.987	113.028	(2,3,4)
		112.161	112.581	(1,2,3)
C=C–S	111.8 (ring)	111.283	110.947	(3,4,5)
		112.640	112.194	(2,1,5)
S–C–CHO	121.9	121.143	121.780	
C–S–C	92.0	90.929	91.250	
C=C–H	129.2 (ring)	122.737	121.790	(4,3,8)
		124.239	124.174	(3,2,7)
		127.489	127.877	(2,1,6)
C–C–H	115.0 (aldehyde)	113.834	115.504	
C–C=O	123.7	124.918	123.531	
Dihedral angle				
S–C–C=O		−0.0002	180.000	

Table 2
Mulliken atomic charges

		syn	*anti*
1	C	−0.334	−0.335
2	C	−0.096	−0.100
3	C	−0.098	−0.113
4	C	−0.185	−0.189
5	S	0.277	0.311
6	H	0.186	0.184
7	H	0.155	0.153
8	H	0.175	0.156
9	C	0.218	0.230
10	H	0.109	0.113
11	O	−0.405	−0.412

Table 3
Experimental and calculated frequencies (cm^{-1}) of *syn* and *anti* thiophene-2-aldehyde

syn conformer		*anti* conformer	
Exp.	Calc.	Exp.	Calc.
A′			
3121	3139.9	–	3143.4
3099	3110.1	–	3123.2
3086	3095.2	–	3104.1
2821	2810.8	–	2812.6
1705	1710.2	1705	1711.3
1524	1523.5	1519	1519.3
1425	1421.2	1432	1419.2
1380	1379.8	1393	1391.4
1340	1329.1	1358	1346.7
1232	1211.0	1241	1221.5
1211	1192.0	1146	1124.1
1084	1074.9	1079	1070.6
1044	1035.1	1034	1018.8
864	841.5	862	836.5
760	732.5	815	788.0
672	651.4	749	718.6
665	636.0	583	563.8
454	437.4	420	404.8
173	168.0	195	188.3
A″			
990	976.5	–	976.6
911	889.3	–	899.6
834	817.3	844	831.0
720	708.8	718	704.0
566	555.4	–	555.2
471	460.2	464	448.4
257	266.7	238	227.6
122	129.9		138.3

Table 4
Calculated frequencies (cm^{-1}), infrared ($km\,mol^{-1}$) and Raman intensities ($\times 10^{-32}\,cm^2\,sr^{-1}$) of *syn* and *anti* thiophene-2-aldehyde conformers

syn conformer			*anti* conformer		
Frequency	IR int.	Raman int.	Frequency	IR int.	Raman int.
3139.9	0.72	152.50	3143.4	0.65	152.70
3110.1	5.01	137.14	3123.2	0.69	95.90
3095.2	3.79	80.45	3104.1	4.25	103.40
2810.8	121.30	155.80	2812.6	114.64	113.10
1710.2	290.42	95.70	1711.3	246.06	94.13
1523.5	12.60	5.00	1519.3	45.30	9.92
1421.2	71.91	118.33	1419.2	65.10	115.00
1379.8	1.08	6.70	1391.4	23.10	40.80
1329.1	0.52	19.58	1346.7	36.00	19.60
1211.0	1.75	4.18	1221.5	56.11	1.19
1192.0	86.42	5.80	1124.1	22.16	1.00
1074.9	2.08	11.99	1070.6	0.29	14.35
1035.1	21.82	1.70	1018.8	22.80	0.41
976.5	0.31	7.58	976.6	0.46	5.59
889.3	0.64	1.22	899.6	1.25	1.35
841.5	5.72	4.13	836.5	15.20	2.90
817.3	6.39	0.81	831.0	6.50	1.86
732.5	18.53	2.81	788.0	44.50	13.80
708.8	58.89	1.74	718.6	3.10	9.90
651.4	10.30	15.35	704.0	59.30	1.77
636.0	26.29	12.40	563.8	16.50	5.04
555.4	0.74	0.04	555.2	1.18	0.02
460.2	4.61	2.84	448.4	3.33	1.13
437.4	0.02	5.12	404.8	1.90	7.11
266.7	7.61	0.59	227.6	7.90	1.66
168.0	6.19	0.43	188.3	5.90	0.45
129.9	2.29	2.07	138.3	3.90	1.42

Raman activity, the strongest bands are at about 3100 and at 1419 cm^{-1}, in excellent agreement with bands of high activity assigned in Ref. [3] to the *syn* conformer at 3099 cm^{-1} and at about 1420 cm^{-1}. Bands reported as strong for this conformer in Ref. [3] at 1215 cm^{-1} (IR), 747 cm^{-1} (IR), 672 cm^{-1} (R), and 1340 cm^{-1} (R), are calculated with a medium intensity in this work.

With regard to the *anti* conformer the most intensive infrared bands are calculated at 2811, 1710, 1421 and 1192 cm^{-1}, and again over 2800, at 1710 and 1421 cm^{-1} for the Raman spectrum. Thus, the actual level of calculation could be used to give insight in the proper assignment of the distinct IR and Raman normal modes for these conformers in combination with potential energy distribution (PED) (see below, Tables 7–10).

3.3. Force constants

The DFT calculated diagonal force constants are presented in Table 5 and selected interaction force constants are given in Table 6. Traditional normal coordinate analysis based on the Wilson GF methodology [24] for predicting valence force fields involves transferring individual force constants of a potential field to the new system and assumes that neglected or unknown force constants are unimportant. For larger molecules and those containing conjugated ring groups these assumptions usually do not hold well enough to distinguish all of the fundamentals in the spectra. One of the most commonly employed strategies to reduce the number of off-diagonal elements is to neglect the stretch–stretch interaction constants that do not include an atom in common. However, it has been pointed out that in the case of conjugated systems, this kind of non-diagonal force constant is important [25]. This fact has been convincingly supported by Neto at al. [26] in their studies of the vibrational spectra of polycyclic aromatic hydrocarbons. Concerning the differences

Table 5
Calculated force constants: diagonal elements

		syn	*anti*
Stretch (mdyn/Å)			
R1	R(1,2)	5.304	5.279
R2	R(2,3)	4.396	4.425
R3	R(3,4)	5.184	5.197
R4	R(4,5)	3.038	3.044
R5	R(1,5)	2.872	2.806
R6	R(1,6)	5.827	5.840
R7	R(2,7)	5.726	5.725
R8	R(3,8)	5.695	5.774
R9	R(4,9)	5.126	5.044
R10	R(9,10)	4.725	4.732
R11	R(9,11)	12.967	12.952
Bend (mdyn Å/rad^2)			
B1	B(2,1,5)	0.637	0.638
B2	B(2,1,6)	0.748	0.744
B3	B(5,1,6)	0.410	0.407
B4	B(1,2,3)	0.400	0.400
B5	B(1,2,7)	0.639	0.640
B6	B(3,2,7)	0.401	0.401
B7	B(2,3,4)	0.402	0.392
B8	B(2,3,8)	0.762	0.766
B9	B(4,3,8)	0.398	0.391
B10	B(3,4,5)	0.479	0.481
B11	B(3,4,9)	1.073	1.070
B12	B(5,4,9)	0.425	0.424
B13	B(1,5,4)	0.480	0.484
B14	B(4,9,10)	0.446	0.467
B15	B(4,9,11)	0.633	0.653
B16	B(10,9,11)	0.536	0.546
Wag–torsion (mdyn Å/rad^2)			
T1	T(5,1,2,3)	0.063	0.063
T2	T(5,1,2,7)	0.042	0.042
T3	T(6,1,2,3)	0.043	0.042
T4	T(6,1,2,7)	0.043	0.037
T5	T(2,1,5,4)	0.038	0.053
T6	T(6,1,5,4)	0.053	0.036
T7	T(1,2,3,4)	0.036	0.038
T8	T(1,2,3,8)	0.037	0.033
T9	T(7,2,3,4)	0.031	0.050
T10	T(7,2,3,8)	0.052	0.033
T11	T(2,3,4,5)	0.035	0.035
T12	T(2,3,4,9)	0.027	0.028
T13	T(8,3,4,5)	0.052	0.051
T14	T(8,3,4,9)	0.035	0.034
T15	T(3,4,5,1)	0.046	0.045
T16	T(9,4,5,1)	0.029	0.027
T17	T(3,4,9,10)	0.098	0.096
T18	T(3,4,9,11)	0.104	0.106
T19	T(5,4,9,10)	0.101	0.096
T20	T(5,4,9,11)	0.110	0.111

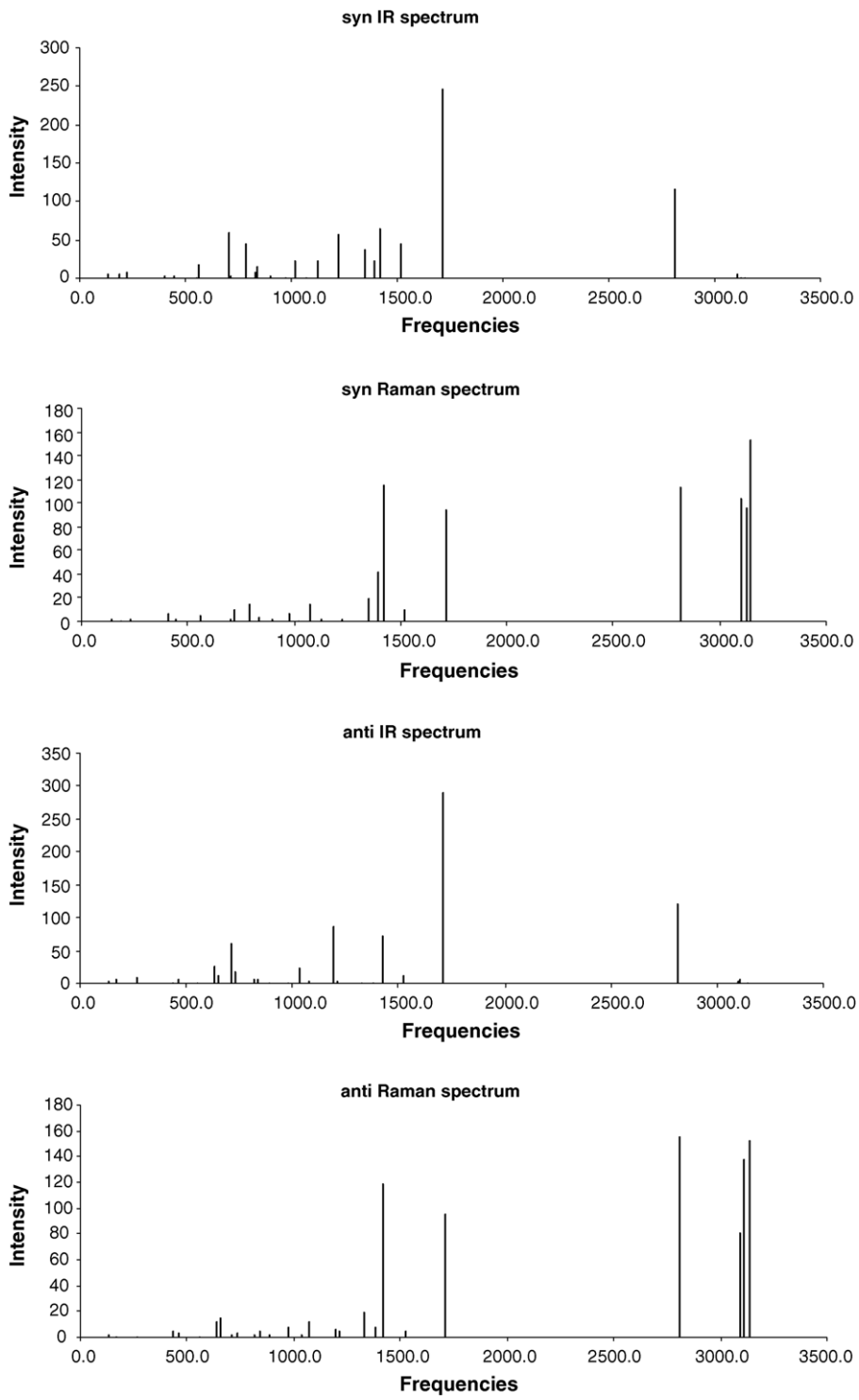

Fig. 2. Simulated infrared and Raman spectra of the *syn* and *anti* conformers of thiophene-2-aldehyde.

with values reported in Ref. [3], we can trust in our results because:

1. GF neglects many off-diagonal force constants;
2. GF does not consider electronic characteristic of bond, different kind of atoms, different neighbors of atoms;
3. GF starts with force constants, transferred from molecules just similar to the one under study;
4. Thus, our ab initio force constants set is complete enough to assure a good interpretation of the quantum mechanic characteristics of the conformers under study.

3.4. Potential energy distribution

The potential energy distribution (PED) of the calculated normal modes for both conformers obtained with the above set of

Table 6
Selected interactions force constants[a]

	syn	*anti*
Stretch/stretch		
R1/R2	−0.145	−0.158
R1/R5	1.712	1.704
R2/R8	0.046	0.041
R2/R3	−0.191	−0.200
R1/R4	−0.147	−0.132
R4/R6	0.038	0.039
R6/R8	−0.006	0.000
R8/R9	−0.011	−0.028
R9/R11	1.105	1.088
R9/R10	0.167	0.185
Stretch/bend (2 atoms in common)		
R1/B1	−0.627	−0.628
R1/B4	0.404	0.405
R2/B3	0.054	0.054
R4/B4	0.016	0.020
R2/B13	−0.060	−0.063
R8/B13	−0.009	−0.003
R8/B12	−0.009	−0.009
R9/B15	0.146	0.155
Stretch/bend (1 atom in common)		
R1/B13	−0.404	−0.421
R1/B7	−0.006	−0.009
R8/B15	0.003	−0.015
R4/B1	−0.064	−0.072
R8/B3	−0.002	−0.003
R8/B14	0.004	0.008
R8/B9	0.054	0.059
Bend/bend (2 atoms in common)		
B4/B1	−0.318	−0.319
B12/B14	0.008	−0.011
B10/B7	0.004	0.011
B11/B14	0.018	0.002
Bend/bend (2 atoms in common)		
B4/B13	−0.078	0.002
B7/B15	−0.005	0.001
B7/B14	−0.002	−0.004
B13/B15	−0.081	0.064
B13/B14	0.077	−0.051

[a] A complete set of these force constants can be obtained from the corresponding author upon request.

force constants are displayed in Tables 7 and 8 for the in-plane vibrations of *syn* conformer and mainly out-of-plane vibrations, respectively. The same data is reported in Tables 9 and 10 for the *anti* conformer.

In these tables, it is observed that thiophene C–H stretchings and different bond stretchings of the aldehyde group are almost pure, while the distinct vibrations concerning the thiophene ring are very mixed in both conformers. This can be attributed to the conjugation in this part of the molecule, and justify the interaction force constants reported in Table 6. This data along with the calculated IR and Raman intensity are useful to give insight for a proper assignment of the distinct normal modes.

3.5. Rotational parameters, relative stability and dipole moments

Experimental and calculated values of rotational parameters are collected in Table 11. Excellent reproducibility of the experimental rotational constants is obtained. Both conformers are asymmetric top. The calculated rotational parameters for the *syn* conformer are indeed more similar to those obtained in the microwave spectroscopy investigation of thiophene-2-aldehyde [3], while those calculated for the *anti* conformer present low values, but following the same trend.

From the optimized geometries, the total energies for the *syn* and *anti* conformers were calculated to be −666.253041 and −666.250870 a.u., respectively. Therefore, at this level of calculation, the *syn* conformer is found to be more stable than the *anti* form by 476 cm^{-1} (1.36 kcal/mol or 5.6 kJ/mol). This result is in agreement with the statement in Ref. [3]. Pethrick and Wyn-Jones [27] determined by ultrasonic relaxation in the pure liquid that the energy difference between the conformers should be less than 6.7 kJ/mol, although from this experiment it is not possible to determine if *syn* or *anti* is the low-energy form.

The calculated dipole moments (Table 12) are in good agreement with the microwave study of Mönning et al. [28] in which only one conformer was found present in the vapor phase with $\mu_a = 3.00$ D and $\mu_b = 1.84$ D. Those values calculated at the present level of theory show that the *syn* conformer has a larger total dipole moment than the *anti* form, and this is consistent with

Table 7
Potential energy distribution of the *anti* conformer: in-plane vibrations

			Atoms (Fig. 1)						Atoms (Fig. 1)			
			h	*k*	*l*	*m*			*h*	*k*	*l*	*m*
3143.4	93%	H–C stretch	6	1	0	0	5%	H–C stretch	7	2	0	0
	0%	H–C stretch	8	3	0	0	0%	C–C stretch	2	1	0	0
3123.2	87%	H–C stretch	8	3	0	0	9%	H–C stretch	7	2	0	0
	2%	H–C stretch	6	1	0	0	0%	C–C stretch	3	2	0	0
3104.1	84%	H–C stretch	7	2	0	0	11%	H–C stretch	8	3	0	0
	3%	H–C stretch	6	1	0	0	0%	C–C–C bend	1	2	3	0
2812.6	100%	H–C stretch	10	9	0	0	0%	O–C stretch	11	9	0	0
	0%	C–C stretch	9	4	0	0	0%	C–C–O bend	4	9	11	0
1711.3	95%	O–C stretch	11	9	0	0	5%	C–C–H bend	4	9	10	0

Table 7 (*Continued*)

			Atoms (Fig. 1)						Atoms (Fig. 1)			
			h	*k*	*l*	*m*			*h*	*k*	*l*	*m*
	5%	C–C stretch	9	4	0	0	3%	H–C–O bend	10	9	11	0
1519.3	33%	C–C stretch	4	3	0		16%	C–C stretch	2	1	0	0
	8%	C–C stretch	9	4	0	0	7%	C–C–H bend	2	3	8	0
1419.2	22%	C–C stretch	3	2	0	0	21%	C–C stretch	2	1	0	0
	8%	C–C stretch	9	4	0	0	8%	C–C stretch	4	3	0	0
1391.4	29%	H–C–O bend	10	9	11	0	21%	C–C–H bend	4	9	10	0
	8%	C–C stretch	2	1	0	0	5%	O–C stretch	11	9	0	0
1346.7	14%	C–C–H bend	2	1	6	0	12%	S–C–H bend	5	1	6	0
	11%	C–C stretch	3	2	0	0	9%	C–C stretch	2	1	0	0
1221.5	16%	C–C–H bend	4	3	8	0	14%	C–C–H bend	2	3	8	0
	9%	C–C–H bend	1	2	7	0	8%	C–C–H bend	3	2	7	0
1124.1	24%	C–C stretch	9	4	0	0	13%	S–C stretch	5	4	0	0
	7%	C–C stretch	4	3	0	0	7%	C–C–H bend	4	3	8	0
1070.6	22%	C–C–H bend	2	1	6	0	21%	S–C–H bend	5	1	6	0
	10%	C–C stretch	2	1	0	0	9%	C–C–H bend	1	2	7	0
1018.8	18%	C–C stretch	3	2	0	0	17%	C–C–H bend	2	3	8	0
	8%	C–C stretch	9	4	0	0	7%	C–C–H bend	1	2	7	0

Table 8
Potential energy distribution of the *anti* conformer: mainly out-of-plane vibrations

			Atoms (Fig. 1)						Atoms (Fig. 1)			
			h	*k*	*l*	*m*			*h*	*k*	*l*	*m*
976.6	19%	H–C–C–S w–t	10	9	4	5	9%	H–C–C–C w–t	10	9	4	3
	4%	O–C–C–C w–t	11	9	4	3	0%	C–C–C–H w–t	9	4	3	8
899.6	18%	H–C–C–H w–t	8	3	2	7	11%	H–C–C–H w–t	7	2	1	6
	4%	H–C–C–S w–t	7	2	1	5	3%	C–C–C–H w–t	4	3	2	7
836.5	35%	S–C stretch	5	1	0	0	13%	C–C–S bend	2	1	5	0
	10%	C–C–C bend	1	2	3	0	5%	S–C–H bend	5	1	6	0
831.0	13%	H–C–C–H w–t	7	2	1	6	6%	H–C–C–C w–t	8	3	2	1
	5%	C–C–C–H w–t	9	4	3	8	4%	S–C–C–H w–t	5	4	3	8
788.0	18%	C–C–O bend	4	9	11	0	16%	S–C stretch	5	4	0	0
	6%	C–C stretch	9	4	0	0	6%	C–C stretch	4	3	0	0
718.6	31%	S–C stretch	5	1	0	0	8%	S–C stretch	5	4	0	0
	7%	C–C–C bend	2	3	4	0	7%	C–C–C bend	1	2	3	0
704.0	14%	C–C–C–H w–t	3	2	1	6	9%	C–S–C–H w–t	4	5	1	6
	5%	H–C–C–S w–t	7	2	1	5	4%	C–C–C–H w–t	4	3	2	7
563.8	19%	C–S–C bend	1	5	4	0	18%	S–C stretch	5	4	0	0
	7%	C–C–S bend	2	1	5	0	6%	C–C–S bend	3	4	5	0
555.2	8%	C–C–C–C t	4	3	2	1	6%	O–C–C–C w–t	11	9	4	3
	5%	H–C–C–C w	10	9	4	3	5%	C–C–C–S t	3	2	1	5
448.4	10%	H–C–C–C w–t	10	9	4	3	9%	O–C–C–C w–t	11	9	4	3
	5%	C–S–C–C t	4	5	1	2	4%	C–C–C–S t	3	2	1	5
404.8	21%	C–C stretch	9	4	0	0	16%	S–C stretch	5	4	0	0
	7%	C–C–O bend	4	9	11	0	7%	C–C–S bend	3	4	5	0
227.6	63%	H–C–C–C w	10	9	4	3	60%	O–C–C–C w–t	11	9	4	3
	11%	H–C–C–S w	10	9	4	5	9%	O–C–C–S w	11	9	4	5
188.3	34%	C–C–C bend	3	4	9	0	34%	S–C–C bend	5	4	9	0
	11%	C–C–O bend	4	9	11	0	5%	C–C–H bend	4	9	10	0
138.3	84%	O–C–C–S w–t	11	9	4	5	60%	H–C–C–S w–t	10	9	4	5
	23%	O–C–C–C w–t	11	9	4	3	14%	H–C–C–C w–t	10	9	4	3

w: wagging, t: torsion.

Table 9
Potential energy distribution of the *syn* conformer: in-plane vibrations

			Atoms (Fig. 1)						Atoms (Fig. 1)			
			h	*k*	*l*	*m*			*h*	*k*	*l*	*m*
3139.9	92%	H–C stretch	6	1	0	0	6%	H–C stretch	7	2	0	0
	0%	C–C stretch	2	1	0	0	0%	H–C stretch	8	3	0	0
3110.1	69%	H–C stretch	7	2	0	0	24%	H–C stretch	8	3	0	0
	6%	H–C stretch	6	1	0	0	0%	C–C stretch	3	2	0	0
3095.2	75%	H–C stretch	8	3	0	0	23%	H–C stretch	7	2	0	0
	0%	H–C stretch	6	1	0	0	0%	C–C stretch	4	3	0	0
2810.8	100%	H–C stretch	10	9	0	0	0%	O–C stretch	11	9	0	0
	0%	C–C stretch	9	4	0	0	0%	C–C–O bend	4	9	11	0
1710.2	96%	O–C stretch	11	9	0	0	7%	C–C stretch	9	4	0	0
	4%	C–C–H bend	4	9	10	0	3%	H–C–O bend	10	9	11	0
1523.5	33%	C–C stretch	4	3	0	0	13%	C–C stretch	2	1	0	0
	8%	C–C–H bend	2	3	8	0	6%	C–C stretch	9	4	0	0
1421.2	33%	C–C stretch	2	1	0	0	16%	C–C stretch	3	2	0	0
	8%	C–C stretch	4	3	0	0	7%	C–C–H bend	3	2	7	0
1379.8	21%	H–C–O bend	10	9	11	0	14%	C–C–H bend	4	9	10	0
	13%	C–C stretch	3	2	0	0	4%	C–C–H bend	4	3	8	0
1329.1	12%	C–C–H bend	2	1	6	0	12%	H–C–O bend	10	9	11	0
	10%	S–C–H bend	5	1	6	0	9%	C–C stretch	4	3	0	0
1211.0	20%	C–C–H bend	4	3	8	0	13%	C–C–H bend	2	3	8	0
	9%	C–C stretch	4	3	0	0	6%	C–C–H bend	1	2	7	0
1192.0	46%	C–C stretch	9	4	0	0	11%	S–C stretch	5	4	0	0
	8%	C–C stretch	3	2	0	0	3%	C–C–H bend	4	9	10	0
1074.9	22%	C–C–H bend	2	1	6	0	21%	S–C–H bend	5	1	6	0
	11%	C–C–H bend	1	2	7	0	11%	C–C stretch	2	1	0	0
1035.1	25%	C–C stretch	3	2	0	0	16%	C–C–H bend	2	3	8	0
	8%	C–C–H bend	4	3	8	0	6%	C–C–H bend	3	2	7	0

Table 10
Potential energy distribution of the *syn* conformer: mainly out-of-plane vibrations

			Atoms (Fig. 1)						Atoms (Fig. 1)			
			h	*k*	*l*	*m*			*h*	*k*	*l*	*m*
976.5	21%	H–C–C–C w–t	10	9	4	3	10%	H–C–C–S w–t	10	9	4	5
	4%	O–C–C–S w–t	11	9	4	5	1%	C–C–C–H w–t	9	4	3	8
889.3	16%	H–C–C–H w–t	8	3	2	7	15%	H–C–C–H w–t	7	2	1	6
	5%	H–C–C–S w–t	7	2	1	5	4%	C–C–C–H w–t	4	3	2	7
841.5	31%	S–C stretch	5	1	0	0	13%	C–C–S bend	2	1	5	0
	11%	C–C–C bend	1	2	3	0	6%	S–C–H bend	5	1	6	0
817.3	10%	H–C–C–H w–t	7	2	1	6	7%	H–C–C–C w–t	8	3	2	1
	6%	C–C–C–H w–t	9	4	3	8	6%	S–C–C–H w–t	5	4	3	8
732.5	29%	S–C stretch	5	1	0	0	9%	C–C–C bend	2	3	4	0
	5%	C–C–O bend	4	9	1	10	4%	C–C–C bend	1	2	3	0
708.8	13%	C–C–C–H w–t	3	2	1	6	9%	C–S–C–H w–t	4	5	1	6
	6%	H–C–C–S w–t	7	2	1	5	5%	C–C–C–H w–t	4	3	2	7
651.4	9%	C–S–C bend	1	5	4	0	9%	S–C stretch	5	1	0	0
	8%	C–C–O bend	4	9	11	0	6%	C–C–S bend	2	1	5	0
636.0	56%	S–C stretch	5	4	0	0	7%	C–C stretch	9	4	0	0
	6%	C–C–O bend	4	9	11	0	2%	C–C–H bend	4	9	10	0
555.4	8%	C–C–C–C t	4	3	2	1	5%	C–C–C–S t	3	2	1	5
	4%	S–C–C–C t	5	4	3	2	3%	O–C–C–C w–t	11	9	4	3

Table 10 (*Continued*)

			Atoms (Fig. 1)						Atoms (Fig. 1)			
			h	*k*	*l*	*m*			*h*	*k*	*l*	*m*
460.2	11%	H–C–C–S w–t	10	9	4	5	10%	O–C–C–S w–t	11	9	4	5
	5%	C–S–C–C t	4	5	1	2	4%	C–C–C–S t	3	2	1	5
437.4	19%	C–C stretch	9	4	0	0	10%	C–S–C bend	1	5	4	0
	8%	C–C–S bend	3	4	5	0	7%	C–C–C bend	3	4	9	0
266.7	46%	O–C–C–S w–t	11	9	4	5	45%	H–C–C–S w–t	10	9	4	5
	10%	H–C–C–C w–t	10	9	4	3	10%	O–C–C–C w–t	11	9	4	3
168.0	37%	S–C–C bend	5	4	9	0	30%	C–C–C bend	3	4	9	0
	14%	C–C–C bend	4	9	11	0	7%	C–C–C bend	4	9	10	0
129.9	79%	O–C–C–C w–t	11	9	4	3	57%	H–C–C–C w–t	10	9	4	3
	16%	O–C–C–S w–t	11	9	4	5	9%	C–C–C–C t	9	4	3	2

w: wagging t: torsion.

Table 11
Experimental and calculated rotational parameters (GHz)

	Exp.	Calc.	
		syn	*anti*
A	5.11300	5.04963	4.98767
B	1.88785	1.87437	1.77386
C	1.37874	1.36697	1.30850

Table 12
Experimental and calculated dipole moments (D) with a field-independent basis

	Exp.	Calc.	
		syn	*anti*
μ_a	3.00	3.4298	3.3526
μ_b	1.84	1.8846	−0.2074
μ_c		0.1383	0.1387
μ_{tot}		3.9159	3.3619

the increased relative stability of the *syn* conformer. In fact, some of the earliest works on conformational analysis has shown that the conformation with the larger dipole moment become stabilized due to dipole–dipole interaction. [29,30].

4. Summary

Ab initio computations of force constants and vibrational frequencies are found to be feasible for a proper description of thiophene-2-aldehyde conformers. The combination with infrared and Raman spectroscopy provides a theoretical aid in the assignment of all modes since it will help to determine the true mode ordering in a congested region through a detailed force field. The employed level of theory (B3LYP/6-31G(d)) is sufficiently accurate and yet at the same time not too demanding computationally. The theoretical calculations have permitted an investigation of rotational constants, as well as the dipole moments for the distinct rotamers. The calculated stabilities and dipole moments for *syn* and *anti* are consistent and support quite well the experimental statements of the literature.

Acknowledgements

The authors acknowledge projects 1010867 and 7010867 from FONDECYT for financial support. GDF acknowledges project 010203 from DGI Universidad de Playa Ancha. GDF also thanks to Professor W. Collier for generously providing of FCART01 computer program.

Appendix A

Unscaled and scaled calculated harmonic frequencies (cm^{-1}) of the *syn* and *anti* thiophene-2-aldehyde conformers were shown in Table A1.

Table A1
Unscaled and scaled calculated harmonic frequencies (cm^{-1}) of the *syn* and *anti* thiophene-2-aldehyde conformers

Exp.	B3LYP/6-311G(d,p)			B3LYP/6-31G(d)			SVWN/6-31G(d)			BLYP/6-31G(d)			B3PW91/6-31G(d)		
	IR	Scaled	Int.	IR	Scaled	Int.	IR	Scaled	Int.	IR	Scaled	Int.	IR	Scaled	Int.
anti															
720	728	705	28	732	704	24	705	693	29	700	695	25	734	700	27
815	817	791	17	820	788	18				787	783	20	826	788	16
1241	1259	1219	20	1271	1221	23	1228	1208	22	1232	1224	26	1270	1211	22
1358	1385	1341	15				1383	1360	16	1354	1346	18			
1432	1457	1410	23	1476	1419	26	1482	1457	24	1428	1420	22	1486	1418	28
1519	1561	1511	18	1580	1519	18	1562	1536	24	1515	1506	21	1587	1514	18
1705	1762	1706	100	1780	1711	100	1771	1741	100	1688	1678	100	1797	1714	100
–	2892	2800	42	2926	2813	47	2815	2768	49	2809	2792	62	2935	2800	45

Table A1 (*Continued*)

	B3LYP/6-311G(d,p)			B3LYP/6-31G(d)			SVWN/6-31G(d)			BLYP/6-31G(d)			B3PW91/6-31G(d)		
	Raman	Scaled	Act	Raman	Scaled	Act	Raman	Scaled	Act	Raman	Scaled	Act	Raman	Scaled	Act
anti															
	1385	1341	16												
1393	1428	1382	29	1447	1391	27				1402	1393	26	1447	1380	15
1432	1457	1410	68	1476	1419	75	1482	1457	55	1428	1420	48	1486	1418	81
1705	1762	1706	58	1780	1711	62	1771	1741	53	1688	1678	53	1797	1714	61
–	2892	2800	85	2926	2813	74	2815	2768	73	2809	2792	72	2935	2800	75
–	3205	3102	64	3229	3104	68	3164	3111	60	3141	3122	71	3241	3092	64
–	3222	3119	65	3249	3123	63	3179	3126	67	3163	3144	62	3260	3110	61
–	3243	3139	100	3270	3143	100	3202	3148	100	3185	3166	100	3280	3129	100
	B3LYP/6-311G(d,p)			B3LYP/6-31G(d)			SVWN/6-31G(d)			BLYP/6-31G(d)			B3PW91/6-31G(d)		
	IR	Scaled	Int.	IR	Scaled	Int.	IR	Scaled	Int.	IR	Scaled	Int.	IR	Scaled	Int.
syn															
720	732	709	24	737	709	20	711	699	26	706	702	20	739	705	23
1211	1225	1186	29	1240	1192	30	1254	1233	25	1192	1185	23	1251	1193	27
1425	1459	1412	22	1478	1421	25	1482	1458	21	1429	1420	23	1489	1420	24
1705	1760	1704	100	1779	1710	100	1768	1738	100	1686	1676	100	1796	1714	100
2821	2889	2797	38	2924	2811	42	2824	2777	45	2806	2789	55	2935	2800	41
	B3LYP/6-311G(d,p)			B3LYP/6-31G(d)			SVWN/6-31G(d)			BLYP/6-31G(d)			B3PW91/6-31G(d)		
	Raman	Scaled	Act	Raman	Scaled	Act	Raman	Scaled	Act	Raman	Scaled	Act	Raman	Scaled	Act
syn															
1425	1459	1412	62	1478	1421	76	1482	1458	47	1429	1420	54	1489	1420	75
1705	1760	1704	49	1779	1710	62	1768	1738	47	1686	1676	50	1796	1714	60
2821	2889	2797	100	2924	2811	100	2824	2777	100	2806	2789	100	2935	2800	100
3086	3196	3093	45	3220	3095	52	3155	3103	47	3134	3115	51	3231	3083	50
3099	3211	3108	75	3235	3110	88	3171	3118	84	3148	3129	90	3248	3098	84
3121	3240	3136	85	3266	3140	98	3199	3145	95	3181	3162	95	3277	3126	97

The strongest IR and Raman signals are given, together with their relative intensities.

References

[1] E. Davison, Chem. Rev. 100 (2000) 351.

[2] Pulay, in: K.P. Lawley (Ed.), Ab initio Methods in Quantum Chemistry, Wiley, New York, 1987, p. 241.

[3] O. Braathen, K. Kveseth, C.J. Nielsen, K. Hagen, J. Mol. Struct. 145 (1986) 45.

[4] W.J. Hehre, A Guide to Molecular Mechanics and Quantum Chemical Calculations, Wavefunction, Inc., Irvine, CA, 2003.

[5] E.J. Baerends, O.V. Gritsenko, J. Phys. Chem. A 101 (1997) 5383.

[6] W. Koch, M.C. Holthausen, A Chemist's Guide to Density Functional Theory, 2nd ed., Wiley/VCH, Weinheim, 2001.

[7] L. Collado, E. Tunon, F.J. Silla, Ramírez, J. Phys. Chem. A 104 (2000) 2120.

[8] M. Ceccarelli, M. Lutz, M. Marchi, J. Am. Chem. Soc. 122 (2000) 3532.

[9] A. Zanoun, P. Lagant, G. Vergoten, J. Mol. Struct. 510 (1999) 85.

[10] W.G. Han, K.J. Jalkanen, M. Elstner, S. Suhai, J. Phys. Chem. B 102 (1998) 2587.

[11] M.J. Frisch, G.W. Trucks, H.B. Schlegel, G.E. Scuseria, M.A. Robb, J.R. Cheeseman, J.A. Montgomery Jr., T. Vreven, K.N. Kudin, J.C. Burant, J.M. Millam, S.S. Iyengar, J. Tomasi, V. Barone, B. Mennucci, M. Cossi, G. Scalmani, N. Rega, G.A. Petersson, H. Nakatsuji, M. Hada, M. Ehara, K. Toyota, R. Fukuda, J. Hasegawa, M. Ishida, T. Nakajima, Y. Honda, O. Kitao, H. Nakai, M. Klene, X. Li, J.E. Knox, H.P. Hratchian, J.B. Cross, C. Adamo, J. Jaramillo, R. Gomperts, R.E. Stratmann, O. Yazyev, A.J. Austin, R. Cammi, C. Pomelli, J.W. Ochterski, P.Y. Ayala, K. Morokuma, G.A. Voth, P. Salvador, J.J. Dannenberg, V.G. Zakrzewski, S. Dapprich, A.D. Daniels, M.C. Strain, O. Farkas, D.K. Malick, A.D. Rabuck, K. Raghavachari, J.B. Foresman, J.V. Ortiz, Q. Cui, A.G. Baboul, S. Clifford, J. Cioslowski, B.B. Stefanov, G. Liu, A. Liashenko, P. Piskorz, I. Komaromi, R.L. Martin, D.J. Fox, T. Keith, M.A. Al-Laham, C.Y. Peng, A. Nanayakkara, M. Challacombe, P.M.W. Gill, B. Johnson, W. Chen, M.W. Wong, C. Gonzalez, J.A. Pople, Gaussian '03, Revision B.05, Gaussian, Inc., Pittsburgh, PA, 2003.

[12] J.C. Slater, Quantum Theory of Molecules and Solids, vol. 4, McGraw-Hill, New York, 1974.

[13] S.L. Vosko, L. Wilk, M. Nusair, Can. J. Phys. 58 (1980) 1200.

[14] A.D. Becke, Phys. Rev. A 38 (1988) 3098.

[15] C. Lee, W. Yang, R.G. Parr, Phys. Rev. B 37 (1988) 785.

[16] A.D. Becke, J. Chem. Phys. 98 (1993) 5648.

[17] J.P. Perdew, in: P. Ziesche, H. Eschrig (Eds.), Electronic Structure of Solids, Akademie Verlag, Berlin, 1991.

[18] M.M. Francl, W.J. Pietro, W.J. Hehre, J.S. Binkley, M.S. Gordon, D.J. deFrees, J.A. Pople, J. Chem. Phys. 77 (1982) 3654.

[19] J.B. Foresman, A.E. Frisch, Exploring Chemistry with Electronic Structure Methods, 2nd ed., Gaussian, Inc., Pittsburgh, PA, 1994.

[20] T. Clark, J. Chandrasekhar, G.W. Spitznagel, P.v. Schleyer, J. Comp. Chem. 4 (1983) 294.

[21] M.J. Frisch, J.A. Pople, J.S. Binkley, J. Chem. Phys. 80 (1984) 3265.

[22] A.P. Scott, L. Radom, J. Phys. Chem. 100 (1996) 16502.

[23] W.B. Collier, QCPE Bull. 13 (1993) 19.

[24] B. Wilson, J.C. Decius, P.C. Cross, Molecular Vibrations, McGraw-Hill, New York, 1955.

[25] J.R. Scherer, J. Overend, Spectrochim. Acta A 17 (1961) 719.

[26] N. Neto, M. Scrocco, S. Califano, Spectrochim. Acta A 22 (1966) 1981.
[27] R.A. Pethrick, E. Wyn-Jones, J. Chem. Soc. A (1969) 713.
[28] F. Mönning, H. Dreizler, H.D. Rudolph, Z. Natforsch. A20 (1965) 1323.
[29] S. Mizushima, Structure of Molecules and Internal Rotation, Academic, New York, 1954.
[30] I.M. Watanabe, M. Mizuchima, Y. Masiko, Sci. Pap. Inst. Phys. Chem. Res. Jpn. 40 (1943) 425.